Plant Physiology and Biochemistry 129 (2018) 158–167

Contents lists available at ScienceDirect

Plant Physiology and Biochemistry

journal homepage: www.elsevier.com/locate/plaphy

Research article

Identification of a type II cystatin in *Fragaria chiloensis*: A proteinase inhibitor differentially regulated during achene development and in response to biotic stress-related stimuli

Uri Aceituno-Valenzuela[a], María Paz Covarrubias[a], María Francisca Aguayo[a], Felipe Valenzuela-Riffo[b], Analía Espinoza[a], Carlos Gaete-Eastman[b], Raúl Herrera[b], Michael Handford[a], Lorena Norambuena[a,*]

[a] Plant Molecular Biology Centre, Department of Biology, Faculty of Sciences, Universidad de Chile, Santiago, Chile
[b] Instituto de Ciencias Biológicas, Universidad de Talca, Talca, Chile

ARTICLE INFO

Keywords:
Cystatin
Phytocystatin
Fruit development
Stress
Fragaria chiloensis

ABSTRACT

The equilibrium between protein synthesis and degradation is key to maintaining efficiency in different physiological processes. The proteinase inhibitor cystatin regulates protease activities in different developmental and physiological contexts. Here we describe for the first time the identification and the biological function of the cysteine protease inhibitor cystatin of *Fragaria chiloensis*, FchCYS1. Based on primary sequence and 3D-structural homology modelling, FchCYS1 is a type II phytocystatin with high identity to other cystatins of the *Fragaria* genus. Both the papain-like and the legumain-like protease inhibitory domains are indeed functional, based on in vitro assays performed with *Escherichia coli* protein extracts containing recombinant FchCYS1. *FchCYS1* is differentially-expressed in achenes of *F. chiloensis* fruits, with highest expression as the fruit reaches the ripened stage, suggesting a role in preventing degradation of storage proteins that will nourish the embryo during seed germination. Furthermore, *FchCYS1* responds transcriptionally to the application of salicylic acid and to mechanical injury, strongly suggesting that FchCYS1 could be involved in the response against pathogen attack. Overall these results point to a role for FchCYS1 in diverse physiological processes in *F. chiloensis*.

1. Introduction

Fragaria chiloensis is known as the white or beach strawberry, and belongs to the Rosaceae family. It is an evergreen plant that develops annual white flowers, and produces an exotic pinkish-white, perfumed and sweet edible fruit. *F. chiloensis* grows in North and South America in a wide variety of climates and conditions. Indeed native populations grow in central and southern Chile, Hawaii and along the western coast of North America from California to the Aleutian Islands (Hancock et al., 1999). The ability to adapt to such varied environments points to a high genomic flexibility, involving the activation of multiple molecular programs that have lead to the extensive environmental radiation of *F. chiloensis* populations. It has been reported that *F. chiloensis* found in Chile are even more adaptive than the accessions growing in North America (Hancock et al., 1999). Indeed, this specie is found growing both on sandy beaches and in mountains in Chile, and is able to grow under very high salt content and water stress conditions (Retamales et al., 2005). Furthermore, *F. chiloensis* fruits are less sensitive than the commercial red strawberry *F. x ananassa* to the infections caused by the necrotic fungus *Botrytis cinerea* (González et al., 2013).

However, unraveling the molecular mechanisms that underlie such biologically relevant traits in *F. chiloensis* is challenging, due to the current lack of molecular and genetics tools for the white strawberry. The genome sequence of this octoploid specie has yet to be deciphered, hindering the direct identification of genes using reverse genomic approaches. Genetic tools are also restricted due to the difficulty of obtaining mutants and the lack of transformation protocols. However, these challenges are gradually being overcome, as increasing amounts of DNA sequence information are becoming available (Figueroa et al., 2008; Opazo et al., 2010; Pimentel et al., 2010). Such ventures are beginning to facilitate our understanding of the molecular mechanisms, and their regulation, that confer special phenotypic traits to *F. chiloensis* (Espinoza et al., 2016; Handford et al., 2014). In addition, insights can be gained into the particular and distinctive characteristics of this exotic specie, which has evolved with minimal human intervention.

With the aim of identifying and characterizing candidate genes that

* Corresponding author. Las Palmeras 3425 Ñuñoa, Santiago, Chile.
E-mail address: lnorambuena@uchile.cl (L. Norambuena).

https://doi.org/10.1016/j.plaphy.2018.05.021
Received 23 October 2017; Received in revised form 13 April 2018; Accepted 18 May 2018
Available online 19 May 2018
0981-9428/

could impact development as well as resistance to biotic and abiotic stress, we examined the available transcriptomic data of *F. chiloensis* (Pimentel et al., 2010). This analysis highlighted a sequence with high homology to known cystatins. Cystatins are low molecular weight proteins that directly bind to the active site of cysteine proteases such as papain-like (MEROPS peptidase family C1 (Rawlings et al., 2012),) and legumain-like peptidases (MEROPS peptidase family C13 (Rawlings et al., 2012),), inhibiting their activity (Benchabane et al., 2010; Margis et al., 1998; Turk and Bode, 1991; van Wyk et al., 2016). The interaction with papain-like proteases is via the identified cystatin-like (CY) domain. Cystatins from animals and plants share several structural similarities. However due to some unique motifs, plant cystatins have been classified as a new subfamily, called phytocystatins. The uniqueness refers to a consensus motif located in the characteristic α-helix of the CY domain (Benchabane et al., 2010; Margis et al., 1998). Phytocystatins have been identified and characterized in a variety of plant species (M. Abe et al., 1992; Gaddour et al., 2001; Gholizadeh, 2012; Hwang et al., 2009; Martinez et al., 2005b; Shyu et al., 2011; Valdés-Rodríguez et al., 2007). Their molecular function as a protease inhibitor impacts a broad range of biological functions related to different aspects of plant development and physiology. First, their function in seeds is linked to preventing protein degradation during seed development (K. Abe et al., 1987; M. Abe et al., 1992; Diaz-Mendoza et al., 2016). Cystatins could inhibit proteolysis of storage proteins that will be subsequently used by the developed embryo during germination (Arai et al., 2002; Diaz-Mendoza et al., 2016; Hwang et al., 2009). Another role has been described during the defense response. Indeed cystatin accumulation prevents cell death and the damage produced by biotic responses (Belenghi et al., 2003). Cystatins also inhibit fungal growth although the mechanism is still unclear (Abraham et al., 2006; Martinez et al., 2005b; Shyu et al., 2011; Wang et al., 2008). Also these protease inhibitors are able to act as insecticides causing deleterious effects on herbivorous arthropods and nematodes (Carrillo et al., 2010; Goulet et al., 2008). Phytocystatins have also been linked to abiotic stress tolerance due to their inducible expression under such conditions (Gaddour et al., 2001; Massonneau et al., 2005; Pernas et al., 2000; Valdés-Rodríguez et al., 2007; Zhang et al., 2008) and their ability to confer resistance to drought, heat shock and high salinity (Quain et al., 2014; Van der Vyver et al., 2003; Zhang et al., 2008). Cystatins are involved in stress responses as well as underlying physiological processes, and are thus key proteins to identify and characterize. Here, the identification of the first cystatin protein from *F. chiloensis*, FchCYS1, is described. This protein belongs to the type II phytocystatin family, sharing primary sequence as well as tertiary structure features with other phytocystatins. A signal peptide-lacking version of FchCYS1 efficiently inhibits in vitro the proteolytic activity of both papain and legumain. *FchCYS1* is differentially expressed in achenes at different stages of fruit development and responds to salicylic acid and mechanical stimulus, strongly suggesting a role for FchCYS1 in the physiology and stress responses of *F. chiloensis*.

2. Material and methods

2.1. Plant material and treatments

Fragaria chiloensis fruits and flowers were collected from a commercial field located at Purén, Araucania Region, Chile (latitude 38°.04′8.6″ S; longitude 73°.14'.2.96″ W). Fruits at developmental stages C1-C4 were classified as described in Figueroa et al. (2008). Once collected, fruits were maintained at 4 °C for 12 h, frozen under liquid nitrogen and stored at −80 °C. Achenes were removed from receptacles while fruits were still frozen.

Fresh *F. chiloensis* C4-stage fruits were treated with 100 μM salicylic acid (SA) in a solution containing 60 mM citric acid, 74 mM $NaHPO_4$, 2% DMSO, 5 mM DTT, and 0.1% Tween 20 (pH 4.5) for 10 min at room temperature. Subsequently, the solution was removed, and fruits were left for 6 and 12 h at room temperature. Fully-expanded leaves (approximately 8 cm-wide) of laboratory-propagated *F. chiloensis* plants were mechanically damaged in each of their three leaflets by a single 5 mm-diameter punch. After 6 and 24 h, leaves were collected. Untreated leaves were used as controls. Genomic DNA and total RNA were isolated by the modified CTAB protocol (Porebski et al., 1997). Nucleic acid integrity and concentration were checked by electrophoresis and spectrophotometry (Nano Vue Plus).

2.2. FchCYS1 identification and cloning

F. vesca sequences were obtained from The Plant Genomics Resource Phytozome (phytozome.jgi.doe.gov/pz/portal.html). Sequence alignment was performed using CLUSTALW Omega (www.ebi.ac.uk/Tools/msa/clustal).

The *FchCYS1* open reading frame (ORF) was amplified by PCR using C4 cDNA and from leaf genomic DNA. PCR primers were designed based on *FveCYS v1* (AJ862660.1); forward 5′-GGTCAAAAACCAGACT ATGAAATTG-3′ and reverse 5′-TCAGTGCTCCACCTCCATCTGAT-3′. The *FchCYS1* fragment of 708 bp was cloned into pCR8-TOPO (Invitrogen). Cloned fragments were sequenced by Macrogen Inc. using M13 primers. Afterwards, the fragment without the nucleotide sequence that codifies for the predicted N-terminal signal peptide (SP) of *FchCYS1* was PCR-amplified using the forward primer 5′-GGATCCATG TCCACCCT-3′ and the reverse primer mentioned above. The amplified product was cloned into the plasmids pDESt17 and pDEStHis$_6$MBP using Gateway™ LR Clonase™ for gene expression in *E. coli*.

2.3. Quantification of transcript levels

cDNA was synthesized from DNA-free RNA by the ImProm-II™ Reverse Transcription System (Promega). Transcript level quantification was performed by qPCR using SensiMix SYBR Hi-ROX kit (Bioline) in a Stratagene MX300P (Agilent Technologies) (Aguayo et al., 2013). Specific primers were designed for amplifying a fragment of 90 bp toward the 3′-end of the coding sequence of *FchCYS1*; forward 5′-AGCC TTCAGCAGAAGTCCAA-3′ and reverse 5′-GATGGAAGAGCATGCCA AGT-3`. *FchPR5* transcript levels were detected by using the primers forward 5′-CAAGGAGCCAACAAACAGGTCA-3′ and reverse 5′-CCACC GTCAGCTACGATGTTG-3′ for amplifying a 200 bp fragment. *FchRib314* (5′-ACCGTTGATTCGCACAATTGGTCATCG -3′ and 5′-TACTGCGGGTG CGGC AATCGGACG-3′) and *FaGAPDH* (5′-TCCATCACTGCCACCCAGA AGACTG-3′ and 5′-AGCAGGCAGAACCTTT CCGACAG-3) were used as housekeeping genes in different organs and treatments (Amil-Ruiz et al., 2011).

2.4. Expression of FchCYS1 in Escherichia coli

BL21 *E. coli* strain was transformed by electroporation with the plasmid pDESt17 and pDEStHis$_6$MBP containing the *FchCYS1* sequence. Transformed bacteria were selected using 100 mg/L ampicillin. Selected clones were grown in LB culture media to OD_{600} = 0.5–1.0 and IPTG was added to a final concentration of 1 mM for inducing *FchCYS1* expression. After 8 h at 28 °C, cells were collected, washed and resuspended in lysis buffer (20 mM Tris-HCl (pH 8.0), 1 mM EDTA). DNAase I (6u; Ambion) was added and cells were then sonicated (3 pulses of 3 min each). Soluble protein extracts were collected from the supernatant after 9,000 × g centrifugation. Proteins were quantified (Bradford based protein assay; BioRad), subjected to SDS-PAGE and Coomassie staining for analyzing the presence of an over-accumulated band after IPTG induction. Untransformed BL21 *E. coli* was evaluated for the endogenous protein pattern, and protein extracts were used as control of proteases activity.

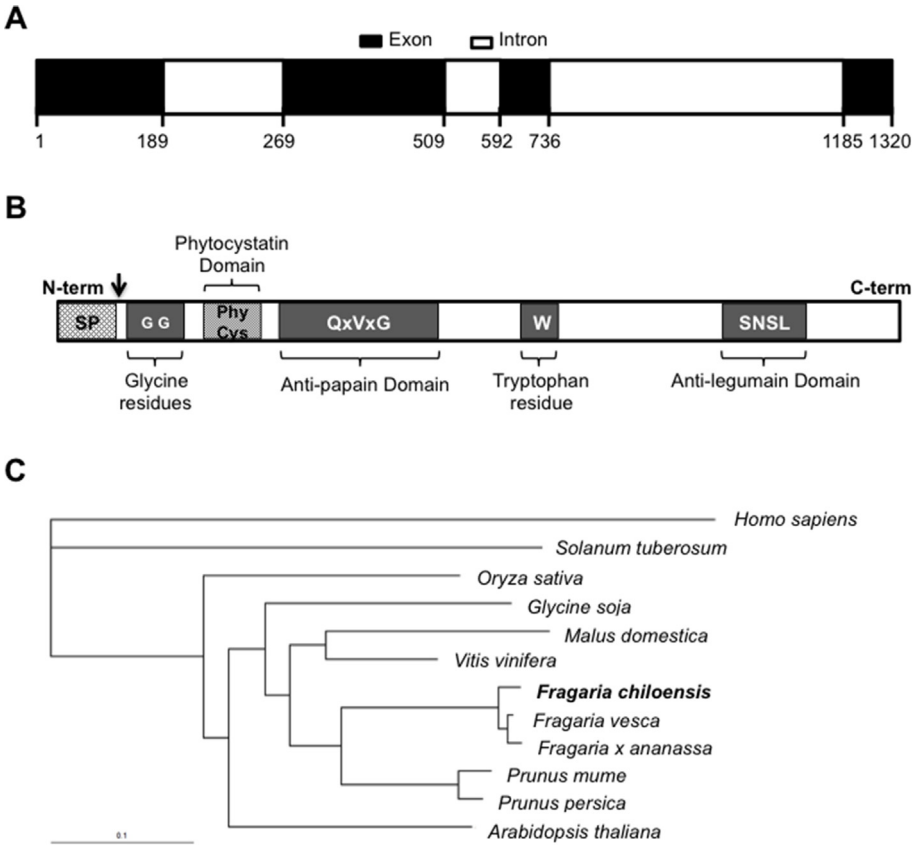

Fig. 1. *FchCYS1* encodes a putative cystatin protein of *F. chiloensis*.
(**A**) Gene intron/exon structure of *FchCYS1*. Genomic and cDNA fragments of the coding region of *FchCYS1* were isolated and sequenced. Numbers indicate the nucleotide positions delimiting exons (black boxes), starting with the codon ATG. (**B**) The deduced FchCYS1 protein sequence (235 aminoacids) contains known motifs involved in the protease-cystatin interaction (gray boxes). A distinctive extended C-terminal tail sequence (SNSL) defines FchCYS1 as a type II cystatin. A signal peptide sequence (SP) and a cleavage site (arrow) are predicted by the SignalP program. The consensus motif (PhyCys) that defines the independent family of phytocystatins is shown. (**C**) A phylogenetic tree was built including FchCYS1 and 10 different type II cystatins with the SNSL motif from rosaceae and non-rosaceae species. *Homo sapiens* cystatin sequence (gi4503107) was used as the root. *Solanum tuberosum* (gi588292978); *Oryza sativa* (gi115435888); *Glycine soja* (gi734347029); *Malus x domestica* (gi27752377); *Vitis vinifera* (gi225464047); *Fragaria vesca* (gi470143070); *Fragaria x ananassa* (gi70907497); *Prunus mume* (gi645281206); *Prunus persica* (gi596049949); *Arabidopsis thaliana* (gi79596870).

2.5. Protease inhibitory activity

Soluble *E. coli* protein extracts were added to the enzymatic reaction for testing FchCYS1 inhibitory activity over papain and legumain. Additionally, IPTG-induced soluble extracts were heated to 100 °C prior to performing the protease inhibition assays. A papain- or legumain-containing reaction without protease inhibitor was considered as 100% activity (control; zero inhibition). The activity of papain (E.C. 3.4.22.2) was measured using as substrate BANA (N-benzoyl-DL-arginine-β-naphthylamide), following a modified protocol from Abe et al. (M. Abe et al., 1992). The enzymatic reaction was performed with 50 μg/mL papain in 10 mM Tris-HCl (pH 8.5), 0.5 mM EDTA and 50 mM 2-mercaptoethanol. The reaction was incubated for 40 min at 37 °C and stopped by adding 2% HCl/ethanol. Then 0.06% ρ-dimethylaminocinnamaldehyde in ethanol was added for color development. After 30 min, absorbance was measured at 540 nm. Legumain activity (E.C. 3.4.22.34) was determined performing a modified protocol from Zakharov et al. (Zakharov, 2004) using Bz-Asn-p-nitroanilide (Bachem) as substrate. The reaction was performed incubating 1 ηg/μL of recombinant human legumain (R&D Systems) in 0.12 M phosphate/citrate (pH 5.6), 0.18 M NaCl, 2 mM DTT and 0.5 mM EDTA for 30 min at 30 °C and stopped afterwards by adding 6% acetic acid. The liberated *p*-nitroaniline was measured at 405 nm.

2.6. The 3D structure of FchCYS1

A signal peptide (SP) prediction was performed with the deduced protein sequence of FchCYS1 that was experimentally obtained from the *FchCYS1* cDNA sequence using SignalP-4.1 server (Petersen et al., 2011) and Phobius (Käll et al., 2004) (Supplementary Fig. S2). BLAST search (Basic local alignment search tool) (Altschul et al., 1997) and PSIPRED (Protein Structure Prediction Server) (Jones, 1999) were performed for selecting the 3D template with the closest homology available in the Brookhaven Protein Data Bank (PDB; http://www.rcsb.org/pdb/home/home.do). The crystal structure of PMC-567, corresponding to the ~35 kDa peptide is composed of three cystatin domains designated 5, 6, and 7 (Green et al., 2013; Nissen et al., 2009) from potato (*Solanum tuberosun*) (PDB: 4LZI) was selected as template, with 43% of sequence identity (*p-value* $6e^{-30}$) and an alignment score of 311 determined by PSIPRED. All bioinformatics parameters were performed as previously reported by Gaete-Eastman et al. (2015).

3. Results and discussion

3.1. Identification of FchCYS1 from Fragaria chiloensis

Partial cDNA sequences identified in *F. chiloensis* fruits (Pimentel et al., 2010) display high similarity to the cystatin gene *Cyf1* characterized in *F. x ananassa* (XM_004307161.2; Martinez et al., 2005b). In order to obtain the full-length sequence of *F. chiloensis* cystatins, the publicly available genome of the closely-related specie *F. vesca* (Shulaev et al., 2011) was used. Taking into account the evolutionary conservation between species belonging to the *Fragaria* genus, the predicted putative type II *F. vesca* cystatin, FveCYS variants 1 and 2, were identified from the database, based on sequence homology to known cystatins. Subsequently, primers for amplifying an open reading frame (ORF) were designed based on the sequence of *FveCYS v1*. Using these primers, a unique band was amplified from ripe fruit cDNA. The isolated fragment was named *FchCYS1*, representing the first cystatin identified in *F. chiloensis* (Gene Bank accession number MH183166). The 708 bp nucleotide sequence of *FchCYS1* (Supplementary Fig. S1) is 98% similar to *FveCYS v1* (AJ862660.1) and 99% similar to the *F. x ananassa Cyf1* (XM_004307161.2; Martinez et al., 2005b).

Phylogenetic analysis has classified cystatins based on their genomic structure, particularly by the number of introns (Margis et al., 1998). The genomic version of the ORF of *FchCYS1* was amplified, using the same primers, from leaf genomic DNA as a fragment of 1320 bp. Comparing the genomic and the cDNA sequence of *FchCYS1* revealed

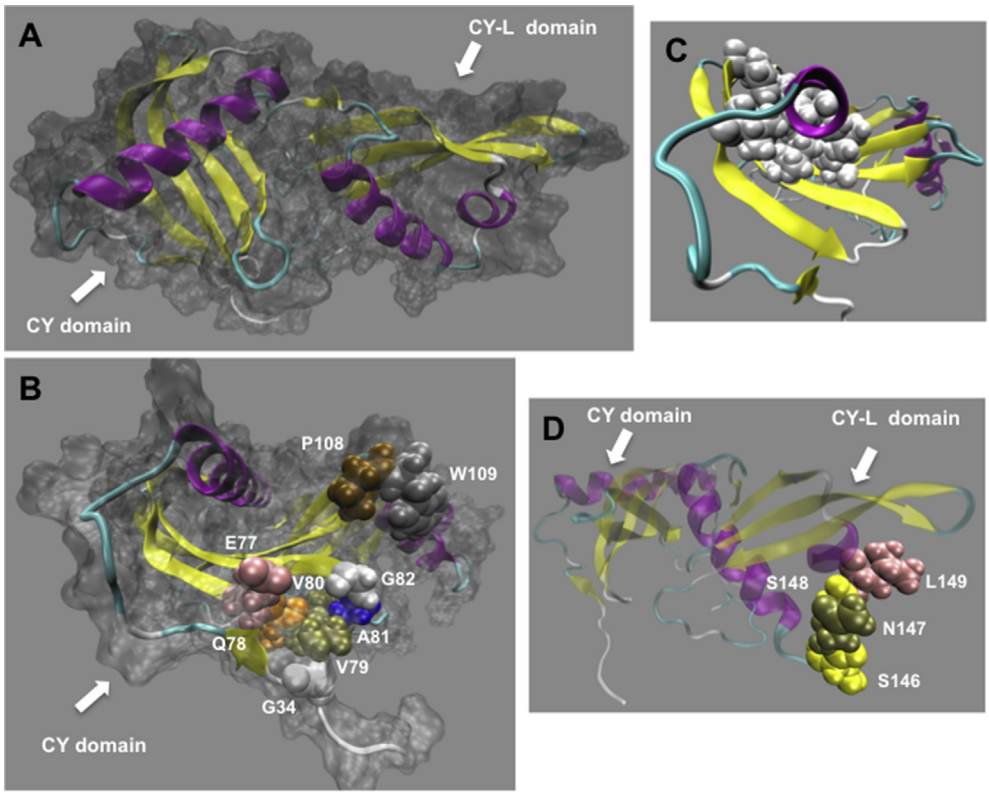

Fig. 2. FchCYS1 identity as a phytocystatin type II is validated by comparative 3D structure modelling.
The predicted mature FchCYS1 sequence was model
ed by comparison to the multicystatin from *Solanum tuberosum* PDB ID code: 4LZI (Green et al., 2013). (**A**) FchCYS1 displays two domains: The inhibitory-papain domain (CY domain) on the left, showing the characteristic αβ roll structure constructed based on one α-helix and four anti-parallels β-strand; and the second domain on the right (CY-L domain) corresponding to the extended C-terminal, showing an incomplete αβ roll structure. The structures of the two domains are shown in both surface representation in gray and colored new cartoon where α-helix (purple), loops (cyan) and β-sheet (yellow) are represented. (**B**) The residues for the interaction with cysteine proteases are shown in a closer view of the CY domain of FchCYS1. Residues are shown in VDW representation. (**C**) The hydrophobic cluster located in the interface between the α-helix and the β-sheet of the CY domain of FchCYS1 is shown. Residues from hydrophobic cluster are colored by charge and shown in VDW representation. (**D**) The SNSL anti-legumain motif was found in an α-helix breaker solvent oriented loop in the CY-L domain of FchCYS1. SNSL residues are shown in VDW representation. (For interpretation of the references to color in this figure legend, the reader is referred to the Web version of this article.)

the presence of three introns interrupting the ORF (Fig. 1A, Supplementary Fig. S1). Most plant cystatin genes possess up to three introns (Margis et al., 1998; Margis-Pinheiro et al., 2008; Martinez et al., 2005a) which is in line with the genomic structure of *FchCYS1*.

After translating the cloned cDNA fragment *in silico*, FchCYS1 is a protein of 235 amino acids, displaying 97.4% identity to FveCYS v1 (Supplementary Fig. S2). Interestingly, primary structure analysis of FchCYS1 revealed a single CY domain with the corresponding three features: Two glycine residues towards the N-terminal (G33 and G34), the tryptophan residue (W109) as well as the papain inhibitory motif QxVxG (Figs. 1B and 2B, Supplementary Fig. S2). Moreover, these three motifs are involved in binding of the cystatin to the active site of papain-like cysteine proteases (Irene et al., 2012). The presence of an extended C-terminal with the SNSL motif has been shown to be critical for inhibition of legumain-like proteases (Martinez et al., 2007), also present in FchCYS1 (S174-L177) classifying it as a type II cystatin (Figs. 1B and 2, Supplementary Fig. S2). The presence of the consensus motif LGRFAVDDHN (Benchabane et al., 2010; Margis et al., 1998) in the primary sequence defined FchCYS1 as a phytocystatin, like most of the cystatins identified so far in plant species (Fig. 1, Supplementary Fig. S2). When comparing the protein sequence of FchCYS1 to other type II cystatins, it was found that FchCYS1 was closely-related to type II cystatins of the *Fragaria* genus (97% sequence identity) and with other members of the Rosaceae family such as *Prunus* spp (72% sequence identity) and *Malus domestica* (74% sequence identity), and more distantly (66 - 62% sequence identity) to orthologues in rice or the known AtCYS6 from *Arabidopsis thaliana* ((Hwang et al., 2009); Fig. 1C, Supplementary Table 1).

The first 28 amino acids of FchCYS1 were predicted with a high score as a putative SP (Fig. 2, Supplementary Fig. S2). This score indicated that FchCYS1 is most-likely synthesized at the endoplasmic reticulum, like cystatins described in carrots, amaranth and jelly fig (Ojima et al., 1997; Shyu et al., 2011; Valdés-Rodríguez et al., 2007). Consequently, this program also predicted a cleavage site for peptidases at the endoplasmic reticulum, strongly suggesting that the functional protein loses its N-terminal region within this compartment (Fig. 1B, Supplementary Fig. S2). However, no glycosylation signals, transmembrane domains or further targeting signals were detected *in silico*. In *Arabidopsis*, seven cystatins have been identified, of which six (AtCYS2-AtCYS7) are predicted to have an SP (Martinez et al., 2005a). The type II cystatin AtCYS6, the closest *Arabidopsis* cystatin to FchCYS1, has been predicted as two different protein products due to alternative splicing of *AtCYS6* (TAIR database). AtCYS6.2, that possesses the SP, is predicted to be accumulated in the extracellular space, while isoform AtCYS6.1 which lacks the SP has been detected in the cytoplasm by proteomic approaches. Therefore, most likely FchCYS1 is secreted by the cells, as described for cystatins of carrot and pineapple (Neuteboom et al., 2009; Ojima et al., 1997). Taken together, the genomic and protein characteristics strongly support the identity of *FchCYS1* as a phytocystatin.

3.2. FchCYS1 molecular comparative modelling reveals a conserved type II cystatin 3D structure

In order to confirm that the identified amino acid residues confer functional features in the tertiary structure of FchCYS1, comparative 3D modelling was performed. Additionally, comparative 3D modelling allowed determining the spatial coordinates of highly-conserved and functionally-related amino acids of FchCYS1.

For this purpose, the crystalline structure of PMC-567 was selected as template since it is the experimentally-determined structure with both the highest sequence identity and coverage with respect to FchCYS1 (42% and 82%, respectively) according to a BLASTp search against the Protein Data Bank (PDB; S2 Table). PMC-567 is a multicystatin from *Solanum tuberosum* (PDB ID code: 4LZI (Green et al., 2013),) that has three CY domains, typical of the type III cystatin family. Furthermore, a secondary structure prediction using the PSIPRED tool of the target sequence (FchCYS1) was performed. The analysis

showed that the highest number of residues with defined 2D structure aligned with the PMC-567 structure. Other putative templates showed lower values (around 95–85 residues) and were therefore discarded. More interestingly, the alignment score of PMC-567 has a value of 291, which is similar to the other putative templates (300–291) which cover only half of the FchCYS1 protein sequence (PSIPRED Score, S2 Table). Additionally, FchCYS1 and PMC-567 proteins are predicted to be post-translationally processed by cleavage of the N-terminal SP, and possess moderate identity and similarity (43% and 57%, respectively). In conclusion, PMC-567 resulted to be the most suitable crystalline structure to model FchCYS1 3D structure.

Manual optimization by incorporating information of phytocystatin secondary structure was performed after sequence alignment between FchCYS1 and the template PMC-567. Residues were incorporated especially associated to structural motifs of the CY domain. Different quality parameters were determined, due to the fact that FchCYS1 and PMC-567 showed moderate amino acid identity. An exhaustive geometric and energetic stability evaluation was performed for FchCYS1 (Supplementary Fig. S3). The best conformer was determined by using different evaluation methods of 10 conformers obtained after energy minimization. The favored regions after PROCHECK analysis corresponded to 100% of the structure and no badly-modeled residues were found (Supplementary Fig. S3A). Furthermore, a low ProSA energy score was obtained in most structurally-conserved regions; however a small region corresponding to a loop distant from the anti-papain motif had an unfavorable ProSA energy score (Supplementary Fig. S3B). Finally, Verify3D showed favorable scores for the full 3D protein structure, and no residues showed values under 0, indicating congruence between the 1D and 3D structures. The final FchCYS1 protein structure was geometrically and energetically stable. All parameters measured favored the acceptance of the model for subsequent analysis.

The FchCYS1 model displayed the two domain-like structures proposed for type II cystatins: the cystatin domain (CY; residues 46–121) and the extended cystatin-like domain (CY-L; 148–235), connected by a linker (residues 122–147) (Fig. 2A). FchCYS1 contains an unstructured N-terminus with a short β-strand (residues 29–45), followed by a compact inhibitory domain (CY domain; 46–121). The compact CY domain is composed of one α-helix and four β-sheets classified in the CATH database as an αβ-roll structure, where the α-helix is encircled by antiparallel β-strands (Fig. 2A; CY domain). Interestingly, the C-extension shows an apparently similar folding, with one β-sheet lacking and a particular orientation of the inhibitor domain (Fig. 2A; CY-L domain). The CY domain has three structural motifs that are highly-conserved within the cystatin protein family and which are functionally related to the putative roles of proteinase inhibitors: motif 1; G33, G34, motif 2; E77, Q78, V79, V80, A81, G82, and motif 3; P108 and W109. Additionally, our model included E77 (motif 2) and P108 (motif 3), whose position was fully-conserved within the phytocystatin protein family (van Wyk et al., 2016). Indeed, these two amino acids are the most highly-conserved residues when 332 phytocystatin protein sequences were compared. Moreover, the three motifs of FchCYS1 were located on one side of the CY domain in three loops (Fig. 2B), concordant with other phytocystatin protein family members (van Wyk et al., 2016), suggesting an interaction with papain-like proteases, as has been suggested for cystatins in pineapple and barley (Irene et al., 2012; Martinez et al., 2009). On the other hand, the compact globular structure of the CY domain is stabilized by a hydrophobic cluster composed of residues located at the interface between a β-sheet and an α-helix, as shown in Fig. 2C. The α-helix contained the highly-conserved residues in the phytocystatin protein family; the L51, G52, R53, F54, A55, V56, D57, D58 and N60 motif (Supplementary Fig. S4). Also, several residues from this α-helix interact with the structural counterpart of the hydrophobic cluster composed of F69, V72, L87, V89, A102, V104 and F118 located in the β-sheet (Irene et al., 2012).

The CY-L domain, previously described as a C-terminal extension fold (Fig. 2A) is composed of 3 assembled β-strands and an incomplete fourth β-strand in addition to an α-helix, forming an αß-roll structure (Fig. 2A). Although this extension has some similarities with the CY domain, and most of the sequence motifs could be partially identified, the lack of critical residues suggested that this extension is a degenerated part of a multi domain phytocystatin protein (Martinez et al., 2007). Even though this domain is not conserved and has no inhibitory activity over papain proteases, a second motif (SNSL) was found to inhibit legumain cysteine proteases (Christoff et al., 2016; Martinez et al., 2007). In the FchCYS1 3D model, this second motif was located in a loop oriented towards the solvent, next to an α-helix (Fig. 2D). The appearance of the SNSL motif suggested an inhibitory activity of FchCYS1 against legumain proteases. Therefore, FchCYS1 could be a bifunctional type II cystatin, using the N-terminal CY, and the C-extended SNSL terminal domain to inhibit papain-, and legumain-like proteases, respectively, as found in a rice phytocystatin (Christoff et al., 2016).

3.3. *FchCYS1 inhibits papain and legumain protease activity*

Bioinformatically, both primary sequence and tertiary protein structure analysis indicated that FchCYS1 possesses both a papain and a legumain protease inhibition domains. In order to determine the cystatin inhibitory activity of FchCYS1, the ORF lacking the SP nucleotide sequence of *FchCYS1* was cloned in bacteria expression plasmids (see material and methods section for details). This strategy allowed the IPTG-inducible accumulation of an N-terminal His-tagged fusion protein (pDESt17; FchCYS1-His_6), and an N-terminal maltose binding protein (MBP) fusion protein (pDEStHis$_6$MBP; FchCYS1- His$_6$MBP) in *E. coli*, strain BL21. Expected bands of both FchCYS1-His_6 (26 kDa) and FchCYS1-His$_6$MBP (65 kDa) were detected in soluble protein extracts of transformed *E. coli* strains (Fig. 3A). These bands were not detected in the corresponding extracts from untransformed BL21 cells, strongly supporting their identity as recombinant FchCYS1 (Fig. 3A). FchCYS1-His_6 and FchCYS1-His$_6$MBP accumulated in transformed *E. coli* even without IPTG stimulation, but in much lower quantities than in the IPTG-treated transformed strains. The IPTG-inducible promoter T7 has been shown to be active even in the absence of the inductor (Rosano and Ceccarelli, 2014). Therefore, the leaky expression of FchCYS1-His_6 and FchCYS1-His$_6$MBP could be considered as expected.

The in vitro enzymatic papain assay utilizes the synthetic substrate BANA (N-benzoyl-DL-arginine-β-naphthylamide), and releases an indole group which is quantifiable by spectrophotometry. The ability of the soluble extract from FchCYS1-His_6-and FchCYS1-His$_6$MBP-expressing *E. coli* to inhibit papain proteases was determined. Soluble protein extracts from untransformed *E. coli* did not inhibit papain activity indicating that there was no bacterial activity of cystatin. In fact, a 6% increase in papain activity was detected in both control conditions and in IPTG-treated untransformed bacteria, suggesting the presence of endogenous papain activity or alternatively, a papain inducer component (Supplementary Table 3). Fig. 3B shows that papain activity was inhibited by up to 80% in the presence of soluble extracts containing either FchCYS1-His_6 or FchCYS1-His$_6$MBP (Fig. 3, Supplementary Table 3). Furthermore, papain inhibition increased even further when either FchCYS1-His_6 or FchCYS1-His$_6$MBP transformed bacteria were induced previously with IPTG, suggesting dependency on the abundance of FchCYS1 in the soluble extract. Indeed, the inhibition of papain was dependent on the protein concentration of the total extracts that accumulated FchCYS1 recombinant proteins, strengthening this assertion (Supplementary Table S4). Surprisingly, both FchCYS1-His_6 and FchCYS1-His$_6$MBP were able to inhibit papain enzymatic activity suggesting that His$_6$MBP, a bulky protein of 42 kDa, did not interfere with FchCYS1 activity (Fig. 3B). However, the extract containing FchCYS1-His$_6$MBP produced the same inhibition as the extract containing FchCYS1-His_6 although the different abundance of FchCYS1 proteins were noticeable, suggesting that FchCYS1-His$_6$MBP activity is less efficient (Fig. 3A and B).

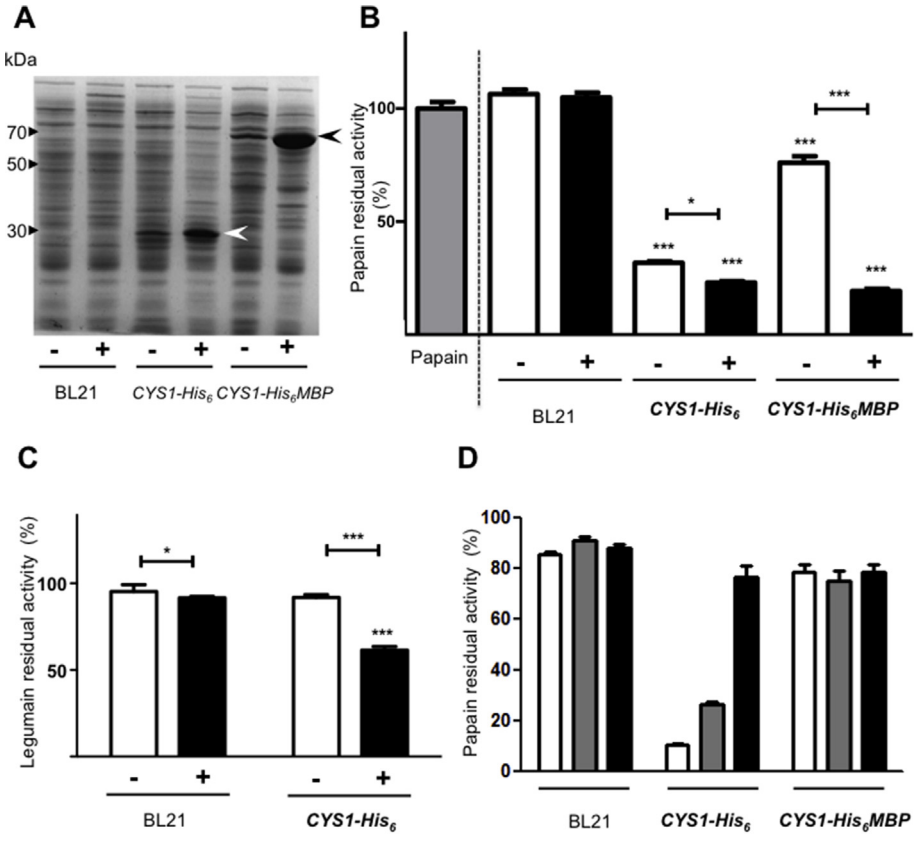

Fig. 3. FchCYS1 has inhibitory activity over papain and legumain proteases.
Soluble protein extracts of BL21 transformed with pDESt17-FchCYS1-His_6 (CYS1- His_6) and pDESt-FchCYS1-His_6MBP (CYS1-His_6MBP) and untransformed BL21, induced (+) or not (−) by IPTG were obtained. (**A**) One hundred μg of protein extracts were subjected to SDS-PAGE and Coomassie staining was performed to visualize proteins. Molecular weight standards are indicated. Proteins of 26 (white arrowhead) and 65 kDa (black arrowhead) are differentially accumulated in the CYS1-His_6 and CYS1- His_6MBP extracts, respectively. (**B-C**) The effect of soluble protein extracts from *E. coli* that accumulated FchCYS1-His_6 and FchCYS1-His_6MBP on papain (**B**) and legumain (**C**) enzymatic activity were evaluated. Transformed and untransformed *E. coli* BL21 strains were treated (+) or not (−) with a final concentration of 1 mM IPTG for inducing recombinant FchCYS1 protein accumulation. Papain and legumain activity were considered 100% in **B** and **C** respectively. Results are informed as the residual activity when the enzymatic assay was performed in presence of 500 μg protein and 50 μg extracts for papain (**B**) and legumain (**C**) activity. Error bars represent standard error (n = 9). One-way ANOVA and Tukey tests were performed *$p \leq 0.05$; **$p \leq 0.01$ and ***$p \leq 0.001$. (**D**) Protein extracts were incubated at 100 °C for a period of time time for analyzing FcCYS1-His_6 and FcCYS1-His_6MBP thermostability over papain activity. Incubations of 10 (white bars), 20 (gray bars), and 60 min (black bars) are shown.

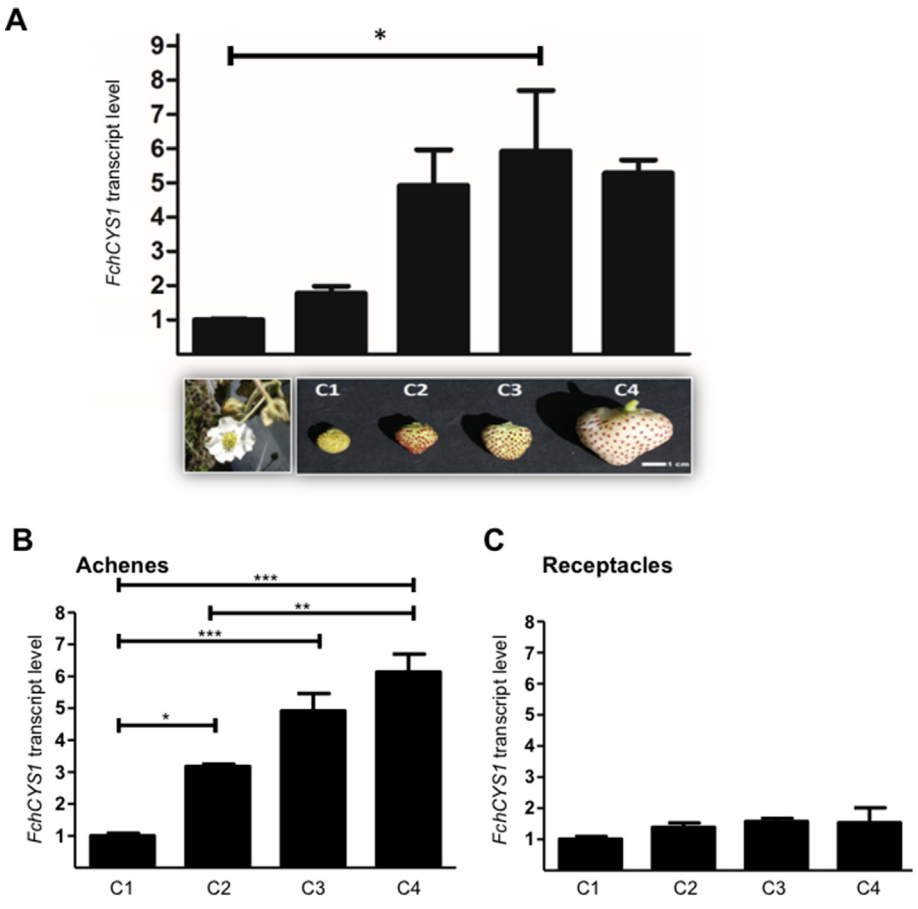

Fig. 4. *FchCYS1* is differentially expressed during fruit development of *Fragaria chiloensis*.
(**A**) *FchCYS1* transcript levels were quantified in flowers and different stages of *F. chiloensis* fruit (C1-C4). C1, green receptacle and green achenes; C2, green receptacle and red achenes; C3, white receptacle and red achenes; and C4, ripe fruits with pink receptacle and red achenes. Representative flower and fruit stages are shown in the image. Bar = 1 cm *FchCYS1* transcript levels were also quantified from achenes (**B**) and receptacles (**C**) collected from C1 to C4 *F. chiloensis* fruits. Transcript levels were measured by means of RT-qPCR. The *FchGAPDH* transcript level was used as normalizer, and the expression level in flowers (**A**), C1-stage achenes (**B**) or C1-stage receptacles (**C**) was used as calibrator. Error bars are shown (n = 9). One-way ANOVA and Tukey tests were performed (*$p \leq 0.05$; **$p \leq 0.01$ and ***$p \leq 0.001$). (For interpretation of the references to color in this figure legend, the reader is referred to the Web version of this article.)

Furthermore, soluble extracts from FchCYS1-His_6 expressing *E. coli* were also able to inhibit the activity of legumain protease (Fig. 3C). The ability of inhibiting legumain protease confirmed the functionality of the extended C-terminal domain containing the SNSL motif (Figs. 1 and 2). Therefore, FchCYS1 was confirmed biochemically as a type II cystatin and is the first identified in *F. chiloensis*.

The inhibition of papain induced by FchCYS1-containing protein extracts was dependent on a temperature-sensitive molecule. The cystatin activity of protein extracts fell when extracts were previously-heated at 100 °C. However, the recombinant protein was partially resistant to temperature treatments, since 60 min of denaturation were necessary to abolish 80% of the enzymatic inhibition over papain (Fig. 3D, Supplementary Table 4). This highlights the thermo-stability of FchCYS1, similar to reported phytocystatins from pineapple and jelly fig (Arai et al., 2002; Shyu et al., 2011, 2004).

3.4. *FchCYS1 is differentially-expressed in achenes during fruit development and responds to biotic and mechanical stimuli*

The stable genetic transformation of *F. chiloensis* has yet to be developed, hindering the generation of mutants or over-expressor lines for the study of the function of specific genes. Therefore, we determined the gene expression pattern of *FchCYS1* in different organs, developmental stages and in response to stimuli, in order to gain insights into the potential physiological roles of this gene.

Cystatins from rice and amaranth have been shown to be involved in inhibition of proteases during embryo development, correlating with protein processing and abundance (K. Abe et al., 1987; Diaz-Mendoza et al., 2016; Valdés-Rodríguez et al., 2007). In order to evaluate the putative role of *FchCYS1*, its transcript levels were measured in fruits at different stages of development. Figueroa et al. (2008) described four distinctive stages of *F. chiloensis* fruit development based on physical features which are related to physiological processes such as achenes ripening, and receptacle coloration and softening. *FchCYS1* transcripts were detected in all four developmental stages (Fig. 4A), in both achenes and receptacles (Fig. 4B and C). *FchCYS1* expression increased during the development of intact fruits (Fig. 4A). This increment arose exclusively from an increase in expression in achenes (Fig. 4B), as levels in receptacles remained constant throughout development (Fig. 4C). This suggests that *FchCYS1* could be involved in inhibiting storage protein degradation during seed development in the Chilean strawberry achenes. Such a finding is consistent with the expression profile observed in the seeds of other plant species, such as rice (K. Abe et al., 1987). The high similarity of *FchCYS1* to the cystatin identified in *F.* x *ananassa* Cyf1 whose expression is detected only in achenes (Martinez et al., 2005b) suggests that the promoter region could contain different information for regulating gene expression in these two closely-related species. Thus, the changes in expression, combined with the inhibitory activity of FchCYS1 shown above, strongly indicate that this protease inhibitor could indeed play a role during the latter stages of fruit/seed development in *F. chiloensis*.

Arabidopsis AtCYS1 and AtCYS2 are expressed in different tissues and organs of plants (Hwang et al., 2010). Indeed, as well as being expressed in fruits (Fig. 4A), *FchCYS1* transcripts are also abundant in flowers (Fig. 4A), and in vegetative tissues such as stolons, roots, and young and old leaves (Fig. 5A). Comparatively, *FchCYS1* transcript levels were more abundant in leaves than in roots and stolons. Furthermore, *FchCYS1* transcript abundance was three times greater in young leaves compared to old leaves. Curiously, whereas transcript levels increased with organ age in reproductive tissues, their levels fell in vegetative tissues (leaves), suggesting that the role of FchCYS1 is not related to general senescence function as has been shown for cystatins of other species (Tajima et al., 2010; van Wyk et al., 2014). On the other hand, higher levels of *FchCYS1* can be interpreted possibly as a preventive mechanism of the plant to cope with the attack of insects and/or pathogens. However, insects produce injuries that trigger a different hormonal cascade. Indeed chestnut cystatin transcript levels respond to wounding as well as fungus infection (Pernas et al., 2000). In order to get insights about such stimuli, the response of *FchCYS1* to mechanical damage was evaluated. The levels of transcript were evaluated when old leaves were hole-punched, provoking and simulating mechanical damage (see materials and methods section). Indeed *FchCYS1* responded, with increasing transcript levels 6 h after the mechanical injury (Fig. 5B). After 24 h, the level of transcript was almost double that in non-stimulated leaves (Fig. 5B).

To determine whether FchCYS1 plays a dual role, both in *F. chiloensis* fruit development and stress responses, as performed by other cystatins (discussed in Introduction section), the transcriptional responses of *FchCYS1* to the phyto-regulator involved in signaling in response to pathogens SA (Glazebrook, 2005) was evaluated. Application of 100 μM SA to mature ripe fruit resulted in a statistically significant increase in *FchCYS1* transcript abundance within 12 h (Fig. 6A). This concentration of SA mimics biotic stress since the SA-responsive *FchPR-5* gene *of F. chiloensis* (González et al., 2013) was also activated. A role for FchCYS1 in defense from pathogens is predicted because gene expression responds to SA and the gene encodes a secreted protein. The role of SA in plant growth and development in response to abiotic stresses has been shown previously. Indeed in *F. x ananassa,* exogenous application of SA improves the deleterious growth due to drought stress (Ghaderi, 2015) implicating also the SA responsiveness genes, including FchCYS1 in the response to cope with abiotic stress.

The transcriptional activation by mechanical damage and application of SA suggest that *FchCYS1* and its gene product are involved in the mechanisms of defence response in *F. chiloensis*.

4. Conclusions

- This work describes the identification of a *F. chiloensis* gene *FchCYS1* that codifies a type II cystatin that shares structural as well as thermodynamic features with described phytocsytatins.
- FchCYS1 expressed as a recombinant protein in *E. coli* indeed possesses inhibitory activity over both papain and legumain proteases, confirming the *in silico* predictions.
- *FchCYS1* is regulated in achenes throughout fruit development and responds to stimuli related with biotic stress.

Funding

This work was mainly-supported by the PBCT Anillo ACT-1110, and partly-financed by FONDECYT 1120289 (LN), 1170950 (LN) 1140257 (MH) and 1181198 (MH), and PAIFAC, Support Program for Research of the Faculty of Sciences, Universidad de Chile (LN).

Author contribution

UA-V, MPC, MFA and AE actively designed experimental strategies and performed experiments. FV-R, CG-E and RH were in charge of performing protein-modelling analysis and interpretations. LN was in charge of compiling data and writing the manuscript. UA-V, CG-E, MH and RH critically reviewed the manuscript. MH and LN led the research.

Conflicts of interest

Authors declare no competing interest.

Acknowledgements

We thank members of the Plant Molecular Biology Centre, University of Chile for helpful discussions. We specially acknowledge the active contribution of Milagros Bracamonte, Aliosha Figueroa and Sara Zapata.

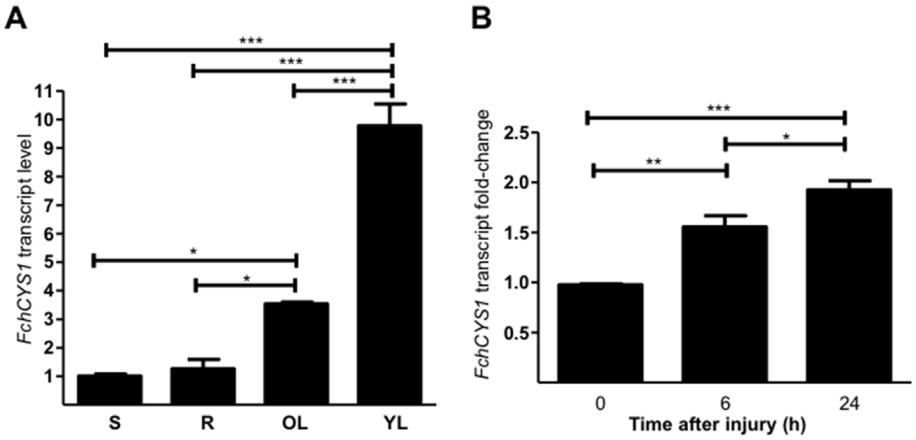

Fig. 5. ***FchCYS1* is induced by mechanical damage in leaves of *Fragaria chiloensis*.**
(**A**). *FchCYS1* transcript levels were quantified in stolons (S), roots (R), old leaves (OL) and young leaves (YL) of *F. chiloensis* plants. (**B**) Fully-expanded leaves of *F. chiloensis* plants were mechanically damaged by a single 5 mm diameter punch in each leaflet. Leaves were collected 6 and 24 h post-injury. *FchCYS1* transcript levels were measured by RT-qPCR. The *FchRib413* transcript was used as a normalizer gene, and expression in stolons (A) and in damaged leaves compared to untreated leaves (B) was used as normalizer. Error bars based on three biological replicates are shown. One-way ANOVA and Tukey tests were performed (*p ≤ 0.05; **p ≤ 0.01 and ***p ≤ 0.001).

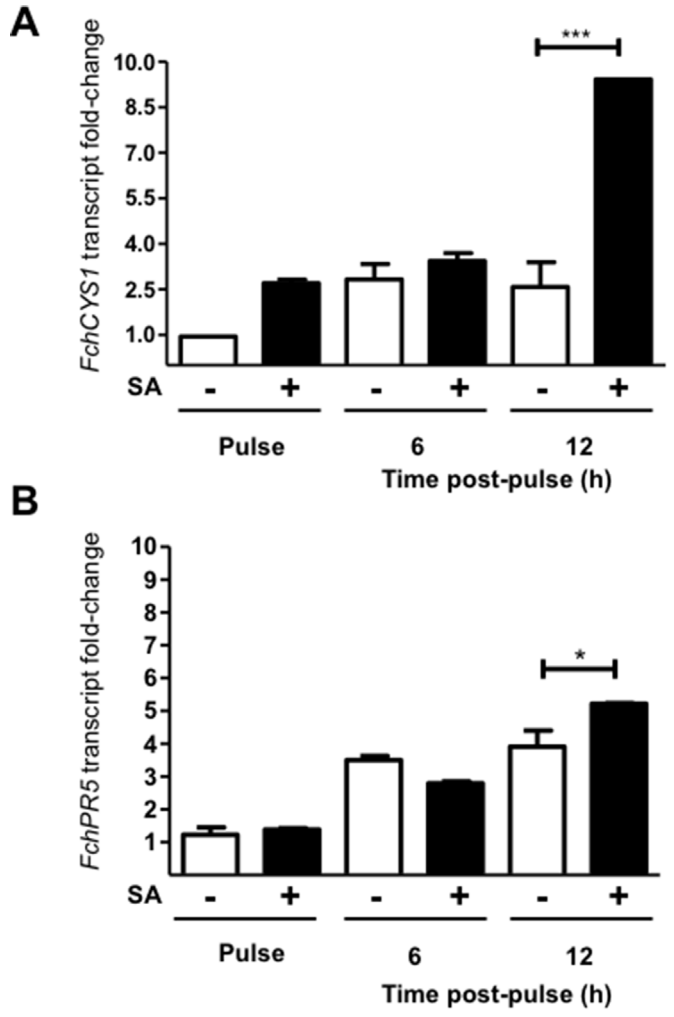

Fig. 6. *FchCYS1* is induced by the application of salicylic acid in fruits of *Fragaria chiloensis.*
F. chiloensis C4-stage fruits were treated with 100 μM salicylic acid (SA) for 10 min (Pulse), and then maintained at room temperature for 6 and 12 h. RNA was isolated from whole treated fruits. *FchPR5* was used as a known SA-responsive gene. (**A**) *FchCYS1* and (**B**) *FchPR5* transcript levels were quantified by means of RT-qPCR. The *FchRIB413* transcript level was used as normalizer, and the expression level in untreated pulse samples was used as calibrator. Error bars are shown (n = 9). One-way ANOVA and Tukey tests were performed (*p ≤ 0.05; **p ≤ 0.01 and ***p ≤ 0.001).

Appendix A. Supplementary data

Supplementary data related to this article can be found at http://dx.doi.org/10.1016/j.plaphy.2018.05.021.

References

Abe, K., Emori, Y., Kondo, H., Suzuki, K., Arai, S., 1987. Molecular cloning of a cysteine proteinase inhibitor of rice (oryzacystatin). Homology with animal cystatins and transient expression in the ripening process of rice seeds. J. Biol. Chem. 262, 16793–16797.

Abe, M., Abe, K., Kuroda, M., Arai, S., 1992. Corn kernel cysteine proteinase inhibitor as a novel cystatin superfamily member of plant origin. Molecular cloning and expression studies. Eur. J. Biochem. 209, 933–937. http://dx.doi.org/10.1111/j.1432-1033.1992.tb17365.x.

Abraham, Z., Martinez, M., Carbonero, P., Diaz, I., 2006. Structural and functional diversity within the cystatin gene family of Hordeum vulgare. J. Exp. Bot. 57, 4245–4255. http://dx.doi.org/10.1093/jxb/erl200.

Aguayo, M.F., Ampuero, D., Mandujano, P., Parada, R., Muñoz, R., Gallart, M., Altabella, T., Cabrera, R., Stange, C., Handford, M., 2013. Sorbitol dehydrogenase is a cytosolic protein required for sorbitol metabolism in Arabidopsis thaliana. Plant Sci. 205–206, 63–75. http://dx.doi.org/10.1016/j.plantsci.2013.01.012.

Altschul, S.F., Madden, T.L., Schäffer, A.A., Zhang, J., Zhang, Z., Miller, W., Lipman, D.J., 1997. Gapped BLAST and PSI-BLAST: a new generation of protein database search programs. Nucleic Acids Res. 25, 3389–3402.

Amil-Ruiz, F., Blanco-Portales, R., Munoz-Blanco, J., Caballero, J.L., 2011. The strawberry plant defense mechanism: a molecular review. Plant Cell Physiol. 52, 1873–1903. http://dx.doi.org/10.1093/pcp/pcr136.

Arai, S., Matsumoto, I., Emori, Y., Abe, K., 2002. Plant seed cystatins and their target enzymes of endogenous and exogenous origin. J. Agric. Food Chem. 50, 6612–6617. http://dx.doi.org/10.1021/jf0201935.

Belenghi, B., Acconcia, F., Trovato, M., Perazzolli, M., Bocedi, A., Polticelli, F., Ascenzi, P., Delledonne, M., 2003. AtCYS1, a cystatin from Arabidopsis thaliana, suppresses hypersensitive cell death. Eur. J. Biochem. 270, 2593–2604. http://dx.doi.org/10.1046/j.1432-1033.2003.03630.x.

Benchabane, M., Schlüter, U., Vorster, J., Goulet, M.-C., Michaud, D., 2010. Plant cystatins. Biochimie 92, 1657–1666. http://dx.doi.org/10.1016/j.biochi.2010.06.006.

Carrillo, L., Martinez, M., Ramessar, K., Cambra, I., Castañera, P., Ortego, F., Diaz, I., 2010. Expression of a barley cystatin gene in maize enhances resistance against phytophagous mites by altering their cysteine-proteases. Plant Cell Rep. 30, 101–112. http://dx.doi.org/10.1007/s00299-010-0948-z.

Christoff, A.P., Passaia, G., Salvati, C., Alves-Ferreira, M., Margis-Pinheiro, M., Margis, R., 2016. Rice bifunctional phytocystatin is a dual modulator of legumain and papain-like proteases. Plant Mol. Biol. 92, 193–207. http://dx.doi.org/10.1007/s11103-016-0504-5.

Diaz-Mendoza, M., Dominguez-Figueroa, J.D., Velasco-Arroyo, B., Cambra, I., González-Melendi, P., Lopez-Gonzalvez, A., Garcia, A., Hensel, G., Kumlehn, J., Diaz, I., Martinez, M., 2016. HvPap-1 C1A protease and HvCPI-2 cystatin contribute to barley grain filling and germination. Plant Physiol. 170, 2511–2524. http://dx.doi.org/10.1104/pp.15.01944.

Espinoza, A., Contreras, R., Zúñiga, G.E., Herrera, R., Moya-León, M.A., Norambuena, L., Handford, M., 2016. FcLDP1, a gene encoding a late embryogenesis abundant (LEA) domain protein, responds to brassinosteroids and abscisic acid during the development of fruits in Fragaria chiloensis. Front. Plant Sci. 7. http://dx.doi.org/10.3389/fpls.2016.00788.

Figueroa, C.R., Pimentel, P., Gaete-Eastman, C., Moya, M., Herrera, R., Caligari, P.D.S., Moya-León, M.A., 2008. Softening rate of the Chilean strawberry (Fragaria chiloensis) fruit reflects the expression of polygalacturonase and pectate lyase genes. Postharvest Biol. Technol. 49, 210–220. http://dx.doi.org/10.1016/j.postharvbio.2008.01.018.

Gaddour, K., Vicente-Carbajosa, J., Lara, P., Isabel-Lamoneda, I., Diaz, I., Carbonero, P.,

2001. A constitutive cystatin-encoding gene from barley (Icy) responds differentially to abiotic stimuli. Plant Mol. Biol. 45, 599–608.
Gaete-Eastman, C., Morales-Quintana, L., Herrera, R., Moya-León, M.A., 2015. In-silico analysis of the structure and binding site features of an α-expansin protein from mountain papaya fruit (VpEXPA2), through molecular modeling, docking, and dynamics simulation studies. J. Mol. Model. 21, 115. http://dx.doi.org/10.1007/s00894-015-2656-7.
Ghaderi, N., 2015. Morpho-physiological responses of strawberry (Fragaria × ananassa) to exogenous salicylic acid application under drought stress. J. Agric. Sci. Technol. 17, 167–178.
Gholizadeh, A., 2012. Molecular analysis of maize cystatin expression as fusion product in Escherichia coli. Physiol. Mol. Biol. Plants 18, 237–244. http://dx.doi.org/10.1007/s12298-012-0119-5.
Glazebrook, J., 2005. Contrasting mechanisms of defense against biotrophic and necrotrophic pathogens. Annu. Rev. Phytopathol. 43, 205–227. http://dx.doi.org/10.1146/annurev.phyto.43.040204.135923.
González, G., Fuentes, L., Moya-León, M.A., Sandoval, C., Herrera, R., 2013. Characterization of two PR genes from Fragaria chiloensis in response to Botrytis cinerea infection: a comparison with Fragaria x ananassa. Physiol. Mol. Plant Pathol. 82, 73–80. http://dx.doi.org/10.1016/j.pmpp.2013.02.001.
Goulet, M.C., Dallaire, C., Vaillancourt, L.P., Khalf, M., Badri, A.M., Preradov, A., Duceppe, M.O., Goulet, C., Cloutier, C., Michaud, D., 2008. Tailoring the specificity of a plant cystatin toward herbivorous insect digestive cysteine proteases by single mutations at positively selected amino acid sites. Plant Physiol. 146, 1010–1019. http://dx.doi.org/10.1104/pp.108.115741.
Green, A.R., Nissen, M.S., Kumar, G.N.M., Knowles, N.R., Kang, C., 2013. Characterization of Solanum tuberosum multicystatin and the significance of core domains. Plant Cell 25, 5043–5052. http://dx.doi.org/10.1105/tpc.113.121004.
Hancock, J.F., Lavín, A., Retamales, J.B., 1999. Our Southern Strawberry Heritage: Fragaria Chiloensis of Chile. HortScience.
Handford, M., Espinoza, A., Bracamonte, M., Figueroa, A., Zapata, S., Aceituno, U., Norambuena, L., 2014. Identification and characterisation of key genes involved in fruit ripening of the Chilean strawberry. N. Biotech. 31, S182. http://dx.doi.org/10.1016/j.nbt.2014.05.912.
Hwang, J.E., Hong, J.K., Je, J.H., Lee, K.O., Kim, D.Y., Lee, S.Y., Lim, C.O., 2009. Regulation of seed germination and seedling growth by an Arabidopsis phytocystatin isoform, AtCYS6. Plant Cell Rep. 28, 1623–1632. http://dx.doi.org/10.1007/s00299-009-0762-7.
Hwang, J.E., Hong, J.K., Lim, C.J., Chen, H., Je, J., Yang, K.A., Kim, D.Y., Choi, Y.J., Lee, S.Y., Lim, C.O., 2010. Distinct expression patterns of two Arabidopsis phytocystatin genes, AtCYS1 and AtCYS2, during development and abiotic stresses. Plant Cell Rep. 29, 905–915. http://dx.doi.org/10.1007/s00299-010-0876-y.
Irene, D., Chung, T.-Y., Chen, B.-J., Liu, T.-H., Li, F.-Y., Tzen, J.T.C., Wang, C.-I., Chyan, C.-L., 2012. Solution structure of a phytocystatin from Ananas comosus and its molecular interaction with papain. PLoS One 7http://dx.doi.org/10.1371/journal.pone.0047865. e47865.
Jones, D.T., 1999. Protein secondary structure prediction based on position-specific scoring matrices. J. Mol. Biol. 292, 195–202. http://dx.doi.org/10.1006/jmbi.1999.3091.
Käll, L., Krogh, A., Sonnhammer, E.L.L., 2004. A combined transmembrane topology and signal peptide prediction method. J. Mol. Biol. 338, 1027–1036. http://dx.doi.org/10.1016/j.jmb.2004.03.016.
Margis, R., Reis, E.M., Villeret, V., 1998. Structural and phylogenetic relationships among plant and animal cystatins. Arch. Biochem. Biophys. 359, 24–30. http://dx.doi.org/10.1006/abbi.1998.0875.
Margis-Pinheiro, M., Zolet, A.C.T., Loss, G., Pasquali, G., Margis, R., 2008. Molecular evolution and diversification of plant cysteine proteinase inhibitors: new insights after the poplar genome. Mol. Phylogenet. Evol. 49, 349–355. http://dx.doi.org/10.1016/j.ympev.2008.04.025.
Martinez, M., Abraham, Z., Carbonero, P., Diaz, I., 2005a. Comparative phylogenetic analysis of cystatin gene families from arabidopsis, rice and barley. Mol. Genet. Genom. 273, 423–432. http://dx.doi.org/10.1007/s00438-005-1147-4.
Martinez, M., Abraham, Z., Gambardella, M., Echaide, M., Carbonero, P., Diaz, I., 2005b. The strawberry gene Cyf1 encodes a phytocystatin with antifungal properties. J. Exp. Bot. 56, 1821–1829. http://dx.doi.org/10.1093/jxb/eri172.
Martinez, M., Cambra, I., Carrillo, L., Diaz-Mendoza, M., Diaz, I., 2009. Characterization of the entire cystatin gene family in barley and their target cathepsin L-like cysteine-proteases, partners in the hordein mobilization during seed germination. Plant Physiol. 151, 1531–1545. http://dx.doi.org/10.1104/pp.109.146019.
Martinez, M., Diaz-Mendoza, M., Carrillo, L., Diaz, I., 2007. Carboxy terminal extended phytocystatins are bifunctional inhibitors of papain and legumain cysteine proteinases. FEBS (Fed. Eur. Biochem. Soc.) Lett. 581, 2914–2918. http://dx.doi.org/10.1016/j.febslet.2007.05.042.
Massonneau, A., Condamine, P., Wisniewski, J.-P., Zivy, M., Rogowsky, P.M., 2005. Maize cystatins respond to developmental cues, cold stress and drought. Biochim. Biophys. Acta Gene Struct. Expr. 1729, 186–199. http://dx.doi.org/10.1016/j.bbaexp.2005.05.004.
Neuteboom, L.W., Matsumoto, K.O., Christopher, D.A., 2009. An extended AE-rich N-Terminal trunk in secreted pineapple cystatin enhances inhibition of fruit bromelain and is posttranslationally removed during ripening. Plant Physiol. 151, 515–527. http://dx.doi.org/10.1104/pp.109.142232.
Nissen, M.S., Kumar, G.N.M., Youn, B., Knowles, D.B., Lam, K.S., Ballinger, W.J., Knowles, N.R., Kang, C., 2009. Characterization of Solanum tuberosum multicystatin and its structural comparison with other cystatins. Plant Cell 21, 861–875. http://dx.doi.org/10.1105/tpc.108.064717.
Ojima, A., Shiota, H., Higashi, K., Kamada, H., Shimma, Y., Wada, M., Satoh, S., 1997. An extracellular insoluble inhibitor of cysteine proteinases in cell cultures and seeds of carrot. Plant Mol. Biol. 34, 99–109.
Opazo, M.A.C., Figueroa, C.R., Henríquez, J., Herrera, R., Bruno, C., Valenzuela, P.D.T., Moya-León, M.A., 2010. Characterization of two divergent cDNAs encoding xyloglucan endotransglycosylase/hydrolase (XTH) expressed in Fragaria chiloensis fruit. Plant Sci. 179, 479–488. http://dx.doi.org/10.1016/j.plantsci.2010.07.018.
Pernas, M., Sánchez-Monge, R., Salcedo, G., 2000. Biotic and abiotic stress can induce cystatin expression in chestnut. FEBS Lett. 467, 206–210. http://dx.doi.org/10.1016/S0014-5793(00)01157-1.
Petersen, T.N., Brunak, S., von Heijne, G., Nielsen, H., 2011. SignalP 4.0: discriminating signal peptides from transmembrane regions. Br. J. Pharmacol. 8, 785–786. http://dx.doi.org/10.1038/nmeth.1701.
Pimentel, P., Salvatierra, A., Moya-León, M.A., Herrera, R., 2010. Isolation of genes differentially expressed during development and ripening of Fragaria chiloensis fruit by suppression subtractive hybridization. J. Plant Physiol. 167, 1179–1187. http://dx.doi.org/10.1016/j.jplph.2010.03.006.
Porebski, S., Bailey, L.G., Baum, B.R., 1997. Modification of a CTAB DNA extraction protocol for plants containing high polysaccharide and polyphenol components. Plant Mol. Biol. Rep. 15, 8–15. http://dx.doi.org/10.1007/BF02772108.
Quain, M.D., Makgopa, M.E., Márquez-García, B., Comadira, G., Fernandez-Garcia, N., Olmos, E., Schnaubelt, D., Kunert, K.J., Foyer, C.H., 2014. Ectopic phytocystatin expression leads to enhanced drought stress tolerance in soybean (Glycine max) and Arabidopsis thalianathrough effects on strigolactone pathways and can also result in improved seed traits. Plant Biotechnol. J 12, 903–913. http://dx.doi.org/10.1111/pbi.12193.
Rawlings, N.D., Barrett, A.J., Bateman, A., 2012. MEROPS: the database of proteolytic enzymes, their substrates and inhibitors. Nucleic Acids Res. 40, D343–D350. http://dx.doi.org/10.1093/nar/gkr987.
Retamales, J.B., Caligari, P.D.S., Carrasco, B., Saud, G., 2005. Current Status of the Chilean Native Strawberry and the Research Needs to Convert the Species into a Commercial Crop 1–2.
Rosano, G.L., Ceccarelli, E.A., 2014. Recombinant protein expression in Escherichia coli: advances and challenges. Front. Microbiol. 5, 172. http://dx.doi.org/10.3389/fmicb.2014.00172.
Shulaev, V., Shulaev, V., Sargent, D.J., Sargent, D.J., Crowhurst, R.N., Crowhurst, R.N., Mockler, T.C., Mockler, T.C., Folkerts, O., Folkerts, O., Delcher, A.L., Delcher, A.L., Jaiswal, P., Jaiswal, P., Mockaitis, K., Liston, A., Liston, A., Mane, S.P., Mane, S.P., Burns, P., Burns, P., Davis, T.M., Davis, T.M., Slovin, J.P., Slovin, J.P., Bassil, N., Bassil, N., Hellens, R.P., Hellens, R.P., Evans, C., Evans, C., Harkins, T., Harkins, T., Kodira, C., Kodira, C., Desany, B., Desany, B., Crasta, O.R., Crasta, O.R., Jensen, R.V., Jensen, R.V., Allan, A.C., Allan, A.C., Michael, T.P., Michael, T.P., Setubal, J.C., Setubal, J.C., Celton, J.-M., Celton, J.-M., Rees, D.J.G., Rees, D.J.G., Williams, K.P., Williams, K.P., Holt, S.H., Holt, S.H., Rojas, J.J.R., Rojas, J.J.R., Chatterjee, M., Chatterjee, M., Liu, B., Liu, B., Silva, H., Meisel, L., Adato, A., Adato, A., Filichkin, S.A., Filichkin, S.A., Troggio, M., Troggio, M., Viola, R., Viola, R., Ashman, T.-L., Ashman, T.-L., Wang, H., Wang, H., Dharmawardhana, P., Dharmawardhana, P., Elser, J., Elser, J., Raja, R., Raja, R., Priest, H.D., Priest, H.D., Bryant, D.W., Bryant, D.W., Fox, S.E., Fox, S.E., Givan, S.A., Givan, S.A., Wilhelm, L.J., Wilhelm, L.J., Naithani, S., Naithani, S., Christoffels, A., Christoffels, A., Salama, D.Y., Salama, D.Y., Carter, J., Carter, J., Girona, E.L., Girona, E.L., Zdepski, A., Zdepski, A., Wang, W., Wang, W., Kerstetter, R.A., Kerstetter, R.A., Schwab, W., Schwab, W., Korban, S.S., Korban, S.S., Davik, J., Davik, J., Monfort, A., Monfort, A., Denoyes-Rothan, B., Denoyes-Rothan, B., Arus, P., Arus, P., Mittler, R., Mittler, R., Flinn, B., Flinn, B., Aharoni, A., Bennetzen, J.L., Bennetzen, J.L., Salzberg, S.L., Salzberg, S.L., Dickerman, A.W., Dickerman, A.W., Velasco, R., Velasco, R., Borodovsky, M., Borodovsky, M., Veilleux, R.E., Veilleux, R.E., Folta, K.M., Folta, K.M., 2011. The genome of woodland strawberry (Fragaria vesca). Nat. Genet. 43, 109–116. http://dx.doi.org/10.1038/ng.740.
Shyu, D.J.H., Chyan, C.-L., Tzen, J.T.C., Chou, W.M., 2004. Molecular cloning, expression, and functional characterization of a cystatin from pineapple stem. Biosci. Biotechnol. Biochem. 68, 1681–1689. http://dx.doi.org/10.1271/bbb.68.1681.
Shyu, D.J.H., Young, Y.M., Lu, H.C., Cheng, Y.M., Tzen, J.T.C., Chou, W.M., 2011. Cloning, functional expression and characterization of a phytocystatin gene from jelly fig (Ficus awkeotsang Makino) achenes. Botanical Studies 52, 407–416.
Tajima, T., Yamaguchi, A., Matsushima, S., Satoh, M., Hayasaka, S., Yoshimatsu, K., Shioi, Y., 2010. Biochemical and molecular characterization of senescence-related cysteine protease-cystatin complex from spinach leaf. Physiol. Plantarum 141, 97–116. http://dx.doi.org/10.1111/j.1399-3054.2010.01425.x.
Turk, V., Bode, W., 1991. The cystatins: protein inhibitors of cysteine proteinases. FEBS Lett. 285, 213–219. http://dx.doi.org/10.1016/0014-5793(91)80804-C.
Valdés-Rodríguez, S., Guerrero-Rangel, A., Melgoza-Villagómez, C., Chagolla-López, A., Delgado-Vargas, F., Martínez-Gallardo, N., Sánchez-Hernández, C., Délano-Frier, J., 2007. Cloning of a cDNA encoding a cystatin from grain amaranth (Amaranthus hypochondriacus) showing a tissue-specific expression that is modified by germination and abiotic stress. Plant Physiol. Biochem. 45, 790–798. http://dx.doi.org/10.1016/j.plaphy.2007.07.007.
Van der Vyver, C., Schneidereit, J., Driscoll, S., Turner, J., Kunert, K., Foyer, C.H., 2003. Oryzacystatin I expression in transformed tobacco produces a conditional growth phenotype and enhances chilling tolerance. Plant Biotechnol. J 1, 101–112. http://dx.doi.org/10.1046/j.1467-7652.2003.00010.x.
van Wyk, S.G., Kunert, K.J., Cullis, C.A., Pillay, P., Makgopa, M.E., Schlüter, U., Vorster, B.J., 2016. Review: the future of cystatin engineering. Plant Sci. 246, 119–127. http://dx.doi.org/10.1016/j.plantsci.2016.02.016.
van Wyk, S.G., Du Plessis, M., Cullis, C.A., Kunert, K.J., Vorster, B.J., 2014. Cysteine protease and cystatin expression and activity during soybean nodule development and senescence. BMC Plant Biol. 14, 294. http://dx.doi.org/10.1186/s12870-014-

0294-3.
Wang, K.-M., Kumar, S., Cheng, Y.-S., Venkatagiri, S., Yang, A.-H., Yeh, K.-W., 2008. Characterization of inhibitory mechanism and antifungal activity between group-1 and group-2 phytocystatins from taro (Colocasia esculenta). FEBS J. 275, 4980–4989. http://dx.doi.org/10.1111/j.1742-4658.2008.06631.x.
Zakharov, A., 2004. A comparative study of the role of the major proteinases of germinated common bean (Phaseolus vulgaris L.) and soybean (Glycine max (L.) Merrill) seeds in the degradation of their storage proteins. J. Exp. Bot. 55, 2241–2249. http://dx.doi.org/10.1093/jxb/erh247.
Zhang, X., Liu, S., Takano, T., 2008. Two cysteine proteinase inhibitors from Arabidopsis thaliana, AtCYSa and AtCYSb, increasing the salt, drought, oxidation and cold tolerance. Plant Mol. Biol. 68, 131–143. http://dx.doi.org/10.1007/s11103-008-9357-x.